Gas diffusion layer from Binchotan carbon and its electrochemical properties for supporting electrocatalyst in fuel cell

by Dedi Rohendi

Submission date: 03-Oct-2022 08:31AM (UTC+0700)
Submission ID: 1914776377
File name: iffusion_layer_from_Binchotan_carbon_and_its_electrochemical.pdf (601.42K)
Word count: 6323
Character count: 33466

AIMS Energy, 10(2): 292–305.
DOI: 10.3934/energy.2022016
Received: 29 January 2022
Revised: 30 March 2022
Accepted: 31 March 2022
Published: 12 May 2022

http://www.aimspress.com/journal/energy

Research article

Gas diffusion layer from Binchotan carbon and its electrochemical properties for supporting electrocatalyst in fuel cell

Nirwan Syarif[1,*], Dedi Rohendi[2], Ade Dwi Nanda[3], M. Try Sandi[3] and Delima Sukma Wati Br Sihombing[3]

[1] Department of Chemistry, Universitas Sriwijaya, Indralaya, Sumsel, Indonesia
[2] Research Center of Excellence for Fuel Cell and Hydrogen, Palembang, Sumsel, Indonesia
[3] Student in Department of Chemistry, Universitas Sriwijaya, Indralaya, Sumsel, Indonesia

* **Correspondence:** Email: nsyarif@unsri.ac.id; Tel: +62711580269.

Abstract: The gas diffusion layer (GDL) in the fuel cell has been made from carbon dispersion electrochemically deposited from binchotan. We prepared GDL by spraying the ink on the surface of the conductive paper. The carbon was then characterized by its crystallography, surface functional groups and size by x-ray diffraction (XRD), FT-IR and PSA instrumentations. Cyclic voltammetry and impedance spectroscopy tests were applied to study the GDL electrochemical characters. Buble drop tests were used to obtain contact angles representing the hydrophobicity of the layer. The electrodeposition/oxidation of binchotan derived carbon dispersion has a crystalline phase in its dot structure. According to particle size analysis, carbon dispersion has an average particle size diameter of 176.7 nm, a range of 64.5–655.8 nm, and a polydispersity index was 0.138. The Nyquist plot revealed that the processes in the GDL matrices as the plot consist of two types of structures, i.e., semicircular curves and vertical (sloping) lines. The GDL electrical conductivity of Vulcan and carbon dots were 0.053 and 0.039 mho cm^{-1}. The contact angle between conductive paper and water was 150.27°; between the gas diffusion layer and carbon Vulcan was 123.28°, and between the gas diffusion layer and carbon dispersion was 95.31°. The surface of the GDL with Vulcan is more hydrophobic than that made with carbon dispersion. In other words, the GDL with carbon dispersion is closer to hydrophilic properties. The results show that the carbon can support the gas diffusion layer for hydrophobic and hydrophilic conditions.

Keywords: energy storage; voltammogram; hydrophobicity; hydrophyllic; membrane electrode assembly; impedance spectroscopy

1. Introduction

The gas diffusion layer (GDL) is a porous carbon-based substrate which is typically layer substrate between the support and the catalyst layer of membrane electrode assembly (MEA) serve as catalyst support and medium for electron transfer. The distribution of fuel at the anode and oxygen at the cathode is facilitated by GDL. The nature of the starting material, i.e., surface functionality, crystalinity and particle size of carbon affects the properties of the GDL, i.e., hydrophobicity, electrochemical, electrical conductivity, and pores, which in turn affects the performance of the fuel cell [1], Gu et al. [2] reported that hydrophobic material can be achieved by using controlled functionalization of carbon nanotubes. Crystalinity of carbon affects both electrochemical and electrical of carbon electrode as reported by Yoo et al. [3]. The electrical conductivity of carbon is expected to be high in order to carry the charge electronically. Carbon particle size is known to greatly affect the pore size of the electrode, therefore it affect the ionic transport [4].

There are some cross factors where the properties described previously affect each other. GDL with low conductivity cause the reactant and product diffuse easily. GDL is made to be porous to allow more ions enter MEA matrix [5]. It promotes charge transfer from the electrolyte to MEA, vice versa. It is suggested that the gradual improvement of the electrochemical performances of carbon electrode is mainly a consequence of the simultaneous increase in conductivity [6].

The layer is currently produced using carbon-based materials such as carbon paper, carbon cloth or carbon nanotubes [7] which is made its pores [8] binding with polymer, such as Polytetrafluoroethylene (PTFE). Schweiss et al. [9] reported that impregnation of hydrophyllic agent such as multiwall carbon nanotubes in GDL can enhancement of proton exchange membrane fuel cell performance. Carbon fiber used in coating GDL gave highest cell voltage under both dry and wet operating conditions [10].

Hydrophobic binder is employed to increase the contact angle with the water, therefore t fuelcell flooding can be prevented [11]. Inversely, the imprenation of hydrophilic carbon material to the GDL control its hydrophobicity. The regulation of hydrophobic - hydrophillic is needed to give a balance between the presence of water and its removal. This setting is required only a few microns in length in the GDL matrix but significantly affects the fuelcell performance and durability [12]. A detailed description of the fuelcell's performance and durability can be found in Borup's article [13].

The use of binchotan in fuelcell and GDL has not been previously reported. The binchotan has conductivity due to its thermal process, typically ~1000 °C [14]. At this temperature, most of fibers in biomass have been converted to graphitic carbon [15]. Preparation of carbon dispersion from binchotan has been reported that electrochemically oxidation of binchotan using strong acid produced carbon with dots structures and aggregates in its aquoeus dispersion [16]. The direct use of dispersion in carbon water can simplify the GDL preparation.

There are several methods to prepare the GDL including casting, spin coating, spraying, electrodeposition and doctor blade [17]. The doctor blade coating method has advantages, especially in control the thickness of the layer [18]. This method gives good results that the layer distributed homogenously throughout the support areas with efficient and accurate steps in the process, compared

with that of the hand painting procedure. The method of making GDL affect the electrochemical activity and electrical conductivity of the electrode [19]. These results can be achieved because the contact between the carbon ink and support run smoothly and evenly. It has been reported that the use of doctor blade methods in preparing GDL show good result for its electrochemical and electrical properties [20].

The electrochemical activity of the GDL can be determined by characterizing the GDL using the cyclic voltammetry (CV) and electrochemical impedance spectroscopy (EIS) methods on potentiostat. The electrical conductivity was calculated from the electrochemical impedance spectroscopic (EIS) measurement data [21] instead of cyclic voltammetry [22]. Buble drop test was used to obtain contact angle representing hydrophobicity. The instrumentations are employed to validate the all properties mentioned in the previously regarding that the binchotan is new material for use in fuel cell.

2. Materials and methods

2.1. Materials

Binchotan was purchased from our local manufacturer in Indralaya, Indonesia. Chemicals were purchased in analytic grade, were carbon black Vulcan XC72R (Cabot) used with no further purification, conductive paper (Avcarb), potassium hyroxide (Merck), sodium hydroxide (Merck), polytetrafluoroethylene (PTFE) emulsion (Merck), Nafion emulsion (Merck), methanol (Merck), Whatmann filter paper no. 42 and distilled water.

2.2. Preparation of carbon and characterization

Carbon preparation was carried out in two stages as reported in our other paper [16]. The first stage is electrolysis and the second is sonification. The electrolysis of the wood binchotan employed two electrodes, i.e., titanium plate and a piece binchotan as anode and cathode. Both electrodes were placed in beaker containing 75 mL of 8 M potassium hydroxide solution as electrolyte. The anode and cathode plates were connected to both poles of 9 volts power supply for 24 hours. This stage produced relatively coarse particle of oxidised carbon. carbon particles are left in solution for second step. The solution was sonicated 2 hours in bath to obtained fine carbon solution for use in preparing GDL.

The carbon was then characterized its crystallography, surface functional groups and size by x-ray diffraction (XRD), FT-IR and PSA instrumentations. Crystallographic characterization was carried out using XRD Rigaku MiniFlex at angle of 20 to 80° with the measured sample in powder form. Surface functionality was determined by using Shimadzu Prestige 21. The size of carbon particle was measured using particle size analyzer (PSA). Several methods can be used in determining particle size, generally using imaging particle analysis [23] instead of PSA. The use of PSA has advantages over other methods because the measurements are carried out in bulk and are measured as a size distribution [24]. PSA uses the principle of dynamic light scattering [25]. The carbon solution was taken 1 mL, put into the cuvette, then the cuvette was irradiated by visible light so that diffraction occurred. Scattered light happens when the light/photon hits small particle to undergo Brownian motion. The particles size and its distribution are determined using second order autocorrelation curve of time scale of the particle motion. The curve is derived from autocorrelation function of light intensity trace during the experiment runs.

2.3. Preparation of the gas diffusion layer

Gas diffusion layer (GDL) was made of carbon, binder, and the support. The carbons used as the matrix of GDL were vulcan and carbon binchotan dispersion. The binder used was PTFE emulsion (Merck), nafion (Merck). The support was conductive paper (Avcarb). Total of 0,2 g carbon was dissolved in 10 mL isopropil alcohol and then added 0,0748 g of nafion, 1.5 mL of isopropyl alcohol and 0.0748 g of Nafion solution were added in the mixture. A 0.293 g of PTFE was added to the mixture, after stirred for 1 hour. The mixture was homogenized for 30 minutes in magnetic stirrer and sonicated for 5 minutes to obtained a homogeneous paste. The pasta poured on to 4 cm x 4 cm support and leveled with doctor blade rolling machine to form layer. The layer was dried in the oven for 30 minutes at 80 °C. The GDL was obtained after heating in the furnace for 3 hours at 350 °C and characterised to study its properties.

2.4. Characterization of the gas diffusion layer

2.4.1. Cyclic voltammetry measurement

Electrochemical characterization of the GDL was studied in a three-electrode set up connected to PGSTAT204 Autolab Metrohm potentiostat. The GDL was working electode. Pt wire and Ag/AgCl were used as counter and reference electrode. The measurement was done in the electrolytes, 25% NaOH without the use of additional current collector. The use of NaOH as electrolyte in electrochemical system was reported in Wei et al. [26]. There is a trade off between the need of electrolyte conductivity and the resistance of electrode corrosion in that concentration [27]. The cyclic voltammetry (CV) method was conducted at scan rates 25 mV s^{-1} to investigate the charge storage mechanism of the electrodes and to calculate their electrochemical surface area. It is expected that the GDL does not show a faradaic process in its voltammogram. Rectangular shape of voltammogram means that only ion adsorption and desorption takes place in the layer [28].

2.4.2. Electrochemical impedance spectroscopy Measurement

Electrochemical impedance spectroscopy was performanced in PGSTAT204 Metrohm Potentiostat combine with the FRA (frequency response analyzer) module. It uses three electrodes, i.e, the GDL was working electrode, Ag/AgCl was reference electrode and Pt wire was counter electrode. The FRA module generates user-defined frequency of AC voltage sine wave superimposed with the small applied DC voltage. The AC voltage and the current components before and after being superimposed were acquired by the two channels of FRA. The phase angle shift and total impedance are two parameters read first. The transfer function, real and imaginary part of impedance, Z" and Z', are next and calculated from available data. The results of data processing are displayed as Bode and Nyquist plots.

The first command is used to perform complete frequency scan. The frequency scanning runs from 1 mHz to 1 MHz to have experimental data. The analysis of the data is usually performed by fitting the experimental data as a circular portion of the Nyquist plot of complete frequency scan with calculated data from the equation [29].

The equation of the electrical circuitry is employed to draw semi-circle plot fitted to the -Z"

versus Z' (nyquist) plot of EIS measurement in Nyquist plot. A circuit model designed by an array of ideal components (resistor R, capacitor C and inductor L) connected in series or parallel to reproduce the experimental EIS spectrum. The plot is interpreted to represent the movement of molecules/particles such as the charge/mass transfer, diffusion, electrochemical double layer, ion adsorption, coating, electrical resistance, corrosion, conductivity, and electrochemical reactions.

2.4.3. Electrical conductivity measurement

The value of the electrical conductivity of gas diffusion layer (GDL) was calculated from the measurement results of electrochemical impedance spectroscopy (EIS) on PGSTAT204 Metrohm Potentiostat. The data obtained in this measurement is Nyguist plot graph using NOVA software where the x-axis is the real resistance and the y-axis is the imaginary resistance. The Nyguist plot is fitted to the equivalent circuit (Figure 1).

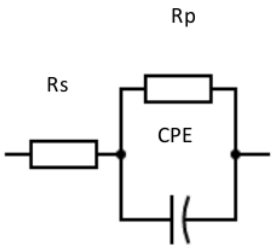

Figure 1. Equivalent circuit for calculating conductivity of gas diffusion layer.

The values for Rp and Rs were obtained from the EIS measurements by using the recorded current response of the electric charge from the electrode interacts with the electrolyte solution [30]. The CPE is the constant phase element that is defined as frequency-independent of capacitive properties for the circuit. Therefore it gives the complexity of capacitance and inductance [31].

The total real resistance (impedance) and conductivity were calculated from EIS data using Eqs 1–3.

$$Z = R_S + \frac{R_P}{1+(\omega t)^2} \quad (1)$$

$$\rho = \frac{Z\,x\,A}{l} \quad (2)$$

$$K = \frac{1}{\rho} \quad (3)$$

Z is the electrical resistance of alternating current (AC) with units of ohm (Ω), is resistance (Ωcm), l is thickness of the layer (cm), A is the surface area (cm^2), and K is conductivity (mho cm^{-1}).

2.2.4. Hydrophobicity measurement

The GDL was placed on the top of plat and clean surface. Digital camera with a macro lens was set to take photos of water droplets from the side as the bubbles can be presented properly. A drop of water was placed on the surface GDL using glass pippete creating buble. The static state of the bubbles was formed shortly after the water droplet contact with GDL surface. Angles between the buble and the surface are varies from one to other depend on surface hydrophobicity. Photos were taken using digital camera with macro lens and processed digitally to produce the best contrast, sharpness and clarity. The contact angle was measured to the photos using On Screen Protractor software.

3. Results

3.1. The carbon dispersion properties

The carbon dispersion was derived from the electrodeposition/oxidation of binchotan using method as described in our other report [16]. The crystallographic characterization of carbon was carried out in the measurement range $2\theta = 0°$ to 80° to the carbon powder after the dispersion was dried. The XRD diffractogram in Figure 2(a) shows the crystallinity as peaks at 2θ = 26.88° and 45.5°. Typical peaks of crystalline carbon appear at 2θ = 24° to 28° for the (001) and 43° to 46° for (110) planes [32]. The (001) plane is the end plane, which plane built the thickness of crystalline carbon, while the (011) is the the broad dimensions of crystalline. The existence of crystalline phase in carbon gives its electrical conductivity.

Colloidal stability of carbon affect its dispersibility and its spreading on the support when carbon ink is sprayed. This spread affects the charge transfer between particles and particles to the support. The colloid particles according to Colloidal Foundations of Nanoscience vary between 1 nm to 1 μm [33]. The analysis of particle size analyzer (PSA) in Figure 2(b) shows the size distribution of the dispersed carbon particles. The distribution of particle size is indicated by the Pdl value (polydispersity index) [34].

The graph states that sample has an average particle size diameter of 176.7 nm, with a polydispersty index (PdI) of 0.138. The PdI has a value range between 0 to 1, for PdI values with a range of 0–0.5 indicating a homogeneous distribution of particles and IdI with a value range of more than 0.5 indicating that the particles have a high level of heterogeneity or polydisperse [35]. It can be seen that the carbon dispersion from binchotan belongs to the nano-micro size. The diameter of the carbon powder particles is measured in the liquid. It can be seen that all particles is in sub-micron, about 1/5 in nano-size. This dispersion condition is affected by the size of carbon particle and the environmental such as solvent and dispersant [36]. If the carbon is not completely dispersed in dispersant, clumping occurs. Clumping causes the particle size to be inconsistent that cause the particles to read larger in PSA measurement [37].

The FTIR spectra (Figure 2(c)) showed the absorption at 1600 cm^{-1}, 1100 cm^{-1}–952.5 cm^{-1} as expected, meaning that carbon in dispersion has C=C aromatic and C=C alkene group in the surface. This functional group is needed to support the charge transfer process that occurs on carbon. The electron cloud at C=C aromatics aids the movement of electrons in the basal plane.

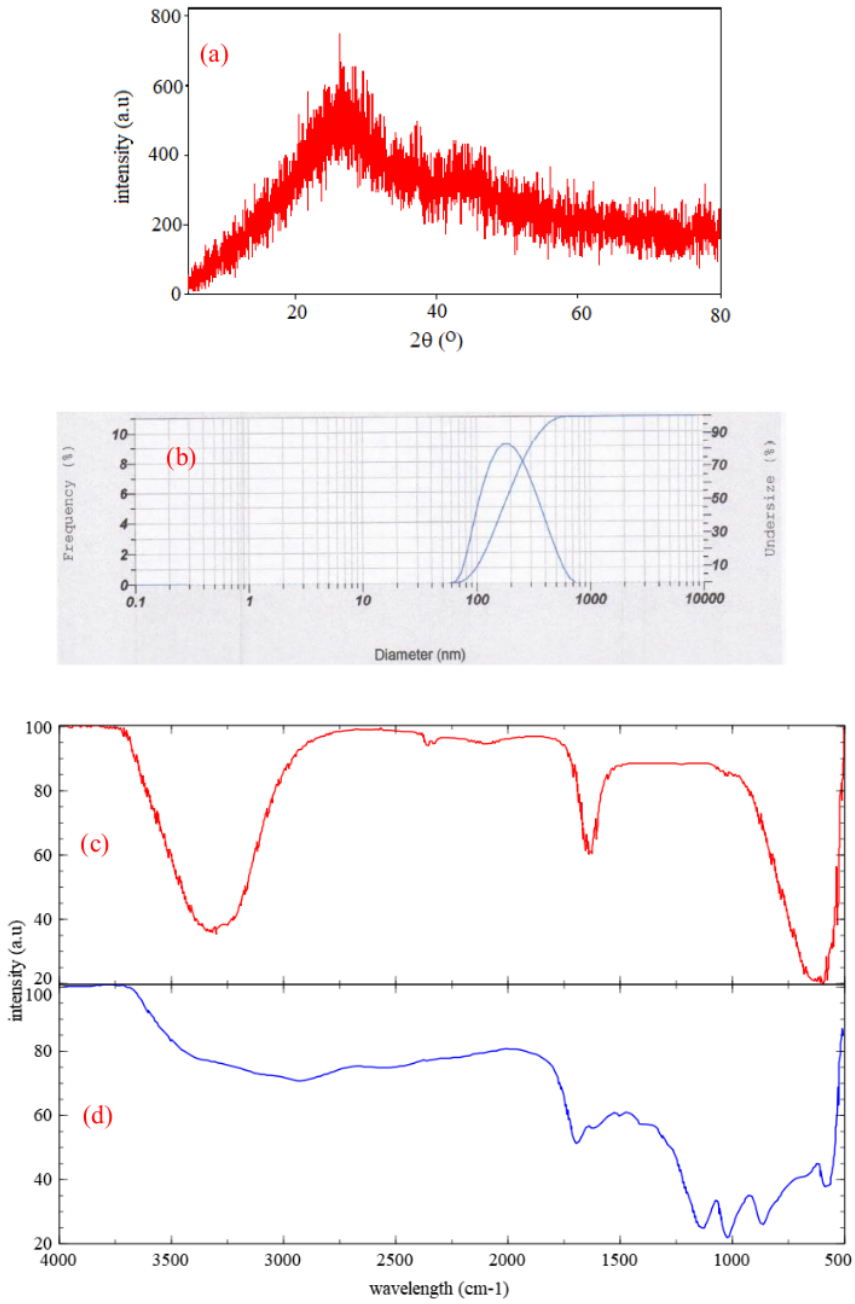

Figure 2. Graph of (a) diffractogram of carbon dispersion, (b) PSA of carbon dispersion, and FTIR spectrogram of (c) carbon vulcan (d) carbon dispersion.

3.2. Morphology of gas diffusion layer

The GDL provides media to gas spreading through all over the area in the surface. The GDL has character that follows the material sprayed on the surface of the conductive paper. The sprayed material or substrate forms single layer (GDL), the other is double layer along with the micro layer [38]. GDL of the carbon binchotan consists of grains that aggregated on a matrix of conductive paper fibers as can be seen from Figure 3 (a). Aggregate are the carbon binchotan covered by solidified electrolyte residue from electro-oxidation process. The electrolyte KOH previously dissolved in the solvent solidified in the drying process. The dark part of the GDL matrix is PTFE which is used as a binder. This explanation has been reported in a previous article [16]. GDL with carbon vulcan has more ordered structure with fiber about 5–10 μm in diameter and pores (Figure 3 (b)). The fiber structure in GDL with vulcan is derived from the original structure of the conductive paper used to form GDL. Dark part in the GDL matrix is PTFE. Pores in layer provide a pathway to promote gas/liquid distribution to other layer.

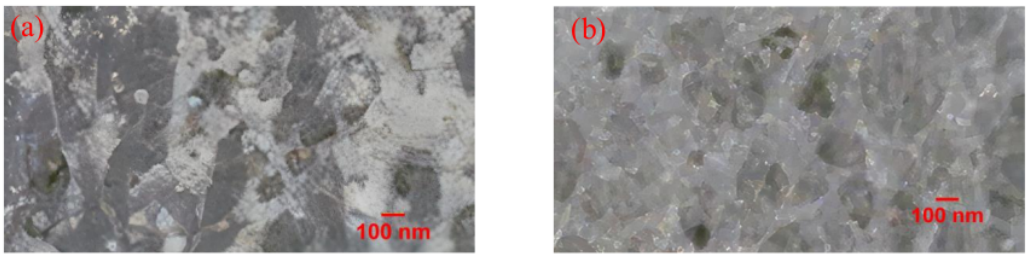

Figure 3. Morphology of gas diffusion layer with support from (a) carbon dots and (b) vulcan.

3.3. Electrochemical character

The existence of the processes in the layer can be seen from size and shape of the curve and peaks in voltammogram. The voltammograms show the processes of reduction, oxidation, and adsorption-desorption process. The measurements were carried out with scan rate 25 mVs^{-1} at half cell of GDL on working electrodes. The GDL has a character fits the character of the material that is sprayed on the surface of the conductive paper. The GDL in a fuel cell can consist of a single layer or a double layer (GDL and micro layer) affecting non-faradaic process which is ionic absorption-desorption.

Figure 4 (a) shows voltammograms of two types of the GDL based on the carbon used. Both voltammograms show no oxidation-reduction process in the potential range of –0.75 to 1 volt. The capacitance of GDL with carbon dispersion measured from the voltammogram is 1/10 of that of GDL with vulcan. The low capacity of GDL with carbon dots is due to the pores of conductive paper being closed by the carbon. Carbon dots in dispersion has tendency to agglomerate. These factors cause the ions in the electrolyte to not be able to enter further, so the charge transfer process is much reduced.

Transport processes in GDL as response to the electric signal can be detected by electrochemical impedance spectroscopy (EIS). The impedance values of these elements are related to real system electrochemical processes such as electron charge transfer, diffusion processes, electrochemical

double layer capacitance determination, ion adsorption mechanism, mass transfer kinetics, and conductivity [39]. This impedance response is commonly observed in electrochemical systems where any chemical species, ions or molecules move towards the surface of electrode due to the applied electric field and are then physically adsorbed on the surface forming an electrochemical double layer..

There are semicircular curves and vertical (sloping) lines exists in the two Nyquist plots (Figure 4(b)). The semicircle on the curve corresponds to a resistance that is primarily determined by its diameter over the entire frequency range, specifically for the charge transfer process, the magnitude is indicated by the diameter of the semicircle in over the entire frequency ranges. [40]. The process is accompanied by second inductance response below the semicircle at low frequency, which means non-faradaic process [41]. A straight line at an angle of 45° to the abscissa means the diffusion of the reactants. Therefore, the Nyquist plot, as shown in Figure 4(b), is typical for coupling between non-electrochemical or electrochemical processes that occur in the layer and a diffusion process.

The diffusion is an important process in GDL. The fuel and oxygen are distributed to carry out electrochemical reactions. The diffusion is affected by materials that build GDL. Carbon binchotan ink has more chemical group functionality [16] that carbon vulcan that make electrolyte interacts with the layer more frequently and diffusion takes place greater.

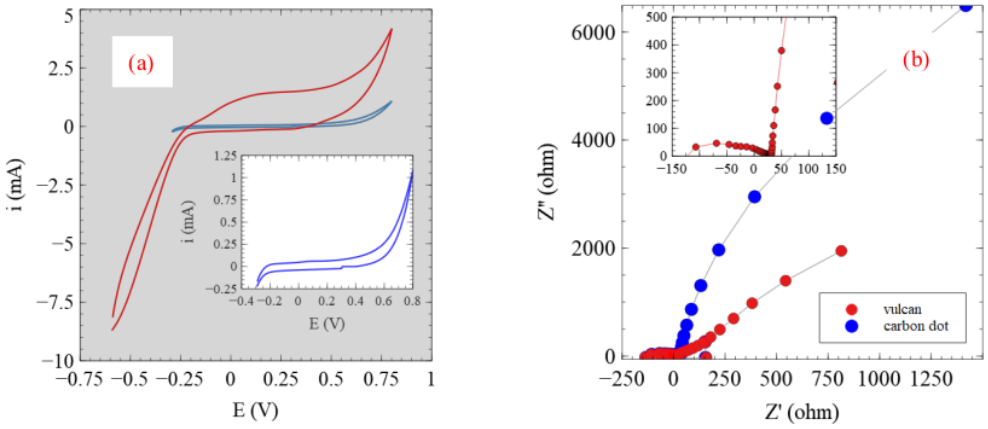

Figure 4. (a) Voltammogram of GDL with carbon vulcan and carbon binchotan (b) Nyquist curve from EIS measurement for GDL with carbon vulcan and carbon binchotan.

Table 1. Conductivity results from the calculation EIS experiments using the model in Figure 1.

No	GDL types	Rs (ohm)	Rp (ohm)	Z (ohm)	K (mho cm^{-1})
1	Conductive paper	−3.102	8.272	5.171	0.129
2	Vulcan	−130.74	143.30	12.56	0.053
3	Carbon binchotan	−128.86	145.81	16.95	0.039

An array of ideal components (resistor R, capacitor C, and inductor L) connected in series or parallel is designed as a circuit model and produces the fitted EIS plot. The Eq (1) is applied to draw a circle or semi-circle contained in the -Z'' versus Z' (Nyquist) plot and fitted to the result of the EIS

measurement to calculate conductivity using Eqs (2) and (3). The results of the conductivity calculation are in Table 1. The conductivity of both GDLs decreased 10–20 times from their support (conductive paper), as carbon binchotan's GDL has the same order as the Vulcan. These values indicate that carbon binchotan meets one of the requirements for GDL.

3.4. Hydrophobicity characteristics

The photograph in Figure 5 determines the contact angle between the water droplet and the GDL surface. The contact angle between the conductive paper and the water droplets is 150.27 as a basis for comparing the changes after being formed into GDL, using carbon binchotan dispersion and Vulcan. The angle between GDL with Vulcan and water droplets is 123.28, and GDL with carbon binchotan and water droplets is 95.31. The carbon paper shows a larger contact angle. The carbon paper used as the primary support material is hydrophobic at first, in case adding a GDL material causes a decrease in the contact angle or is less hydrophobic. The contact angle formed is less hydrophobic. Liquids on the surface of the layer interact with open-chain aliphatic hydrocarbons have low surface tensions. The hydrophobic pores in the GDL can be filled when in contact with this liquid. Water, with relatively high surface tension, fills only the hydrophilic pores. The surface of the GDL with Vulcan is more hydrophobic than that made with carbon dispersion. In other words, the GDL with carbon dispersion is closer to hydrophilic properties. The contact angle of the GDL was determined to be ~90° which indicates the hydrophilic nature of the layers in GDL.

The GDL character in repelling water from crossing both sides of the layer is related to hydrophobicity. On the other hand, when the water enters the opposite side of the MEA, the unwanted process called cross-over happens. This process drains stored electrical charge in ions, as can be inferred from the slopes of the curves in Figure 4. Therefore diffusion in carbon dispersion ran faster than in carbon Vulcan.

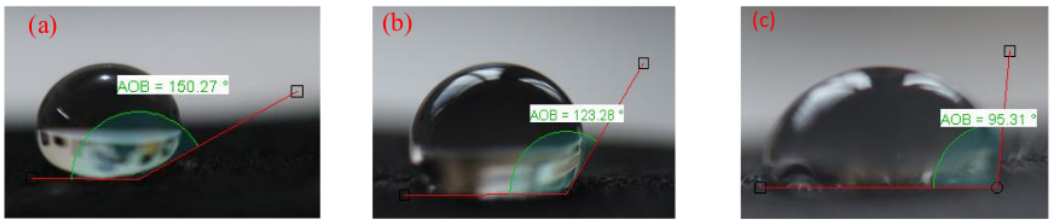

Figure 5. Digitalized photograph of water buble for measuring the contact angle between water and the surface of (a) conductive paper (b) gas diffusion layer with carbon vulcan and (c) gas diffusion layer with carbon dot on conductive paper.

Carbon binchotan or Vulcan and Nafion were mixed and stirred to make ink. Fluorocarbon, such as PTFE, was used as a binder that gives hydrophobic character to the GDL [42]. The ink was sprayed on the surface of the conductive paper (support) to form GDL with some degree of hydrophobicity. The hydrophobic surface of GDL has tension that creates a bubble if water is dropped. The composite of PTFE and proton transfer polymer (Nafion) can be used to produce the required character to get efficient proton transport, such as the balance between water and air transport for regulatory

mechanisms. Removing excess water from GDL makes the path for mass transportation under high operating conditions run smoothly. PTFE treatment is the primary but essential procedure of the GDL substrate preparations, which provides more uniform hydrophobic characteristics that help remove water, i.e., reduces water accumulation to prevent cell flooding and provides more pathways for transport of GDL.

Several treatments are applied to give specific characteristics to the GDL. Most of these treatments make it hydrophobic to avoid flooding in the cell, as seen in GDL with carbon Vulcan (Figure 5(b)). It is explained in other reports that hydrophilic carbon under dry and wet conditions for better liquid/gas diffusivity, largest pore diameter, pore volume to reduce flooding at the cathode and the highest cell voltage [10]. The appropriate coating of hydrophilic material the hydrophobic is effective for reducing flooding in the fuel cell, thereby enhancing the performance [38]. The GDL with hydrophobic-hydrophilic substrates is a promising candidate to handle both ion and electron transfer [43]. Loss of water content in the membrane decreases ionic conductivity, thereby increasing the internal resistance of the cell.

4. Conclusions

The electrodeposition/oxidation of binchotan derived carbon dispersion has a crystalline phase in some nanoscale portions. Carbon binchotan dispersion in water has an average particle size diameter of 176.7 nm, a range of 64.5–655.8 nm and a polydispersity index (PDI) of 0.138 according to the particle size analysis. The carbon dispersion has potence to apply in GDL. The diffusion medium for anode and cathode usually was immersed in PTFE solution and nafion emulsion, followed by drying and sintering to form GDL. The GDL with Vulcan has more pores than carbon dispersion. The GDL of the carbon dispersion consists of grains that are aggregated on a matrix of conductive paper fibers as their support. The Nyquist plot revealed that the processes in the GDL matrices as the plot consist of two types of structures, i.e., semicircular curves and vertical (sloping) lines exists. The GDL electrical conductivity of Vulcan and carbon dots were 0.053 and 0.039 mho cm^{-1}. Electrical conductivity of GDL is needed to ensure better contact between GDL and catalyst layer. The contact angle between conductive paper and water is 150.27°; between GDL and Vulcan carbon, 123.28° and between GDL and carbon dispersion is 95.31°. The surface of the GDL with Vulcan is more hydrophobic than that made with carbon dots. In other words, the GDL with carbon is closer to hydrophilic properties. The application of carbon binchotan shows its potency in supporting the GDL. The appropriate coating of hydrophilic material needs to be developed to make a more effective layer for reducing flooding in the fuel cell, thereby enhancing the performance. Fuel cell generally uses external humidifiers to prevent dehydration of the membrane in its operation. Simplifying the operation of the fuel cell by removing external humidification is a step toward increasing the performance and reducing operating costs.

Acknowledgement

The research/publication of this article was funded by DIPA of Public Service Agency of Universitas Sriwijaya 2021. SP DIPA-023.17.2.677515/2021, On Novermber 23, 2020. In accordance with the Rector's Decree Number: 0010/UN9/SK.LP2M.PT/2021, On April 28, 2021.

Conflict of interest

The authors declare no conflict of interest.

References

1. Chen Y, Jiang C, Cho C (2019) Characterization of effective in-plane electrical resistivity of a gas diffusion layer in polymer electrolyte membrane fuel cells through freeze-thaw thermal cycles. *Energies* 13: 145. https://doi.org/10.3390/en13010145
2. Gu J, Xiao P, Huang Y, et al. (2015) Controlled functionalization of carbon nanotubes as superhydrophobic material for adjustable oil/water separation. *J Mater Chem A* 3: 4124–4128. https://doi.org/10.1039/C4TA07173E
3. Yoo HM, Heo GY, Park SJ (2011) Effect of crystallinity on the electrochemical properties of carbon black electrodes. *Carbon Lett* 12: 252–255. https://doi.org/10.5714/CL.2011.12.4.252
4. Portet C, Yushin G, Gogotsi Y (2008) Effect of carbon particle size on electrochemical performance of EDLC. *J Electrochem Soc* 155: A531. https://doi.org/10.1149/1.2918304
5. Yang L, Li W, Du X, et al. (2010) Effect of hydrophobicity in cathode porous media on PEM fuel cell performance. *J Fuel Cell Sci Technol* 7: 1–6. https://doi.org/10.1115/1.4001051
6. Sánchez-González J, Stoeckli F, Centeno TA (2011) The role of the electric conductivity of carbons in the electrochemical capacitor performance. *J Electroanal Chem* 657: 176–180. https://doi.org/10.1016/j.jelechem.2011.03.025
7. Nagy KA, Tóth IY, Ballai G, et al. (2020) Wetting and evaporation on a carbon cloth type gas diffusion layer for passive direct alcohol fuel cells. *J Mol Liq* 304: 112698. https://doi.org/10.1016/j.molliq.2020.112698
8. Fan L, Tu Z, Chan SH (2021) Recent development of hydrogen and fuel cell technologies: A review. *Energy Rep* 7: 8421–8446. https://doi.org/10.1016/j.egyr.2021.08.003
9. Schweiss R, Steeb M, Wilde PM, et al. (2012) Enhancement of proton exchange membrane fuel cell performance by doping microporous layers of gas diffusion layers with multiwall carbon nanotubes. *J Power Sources* 220: 79–83. https://doi.org/10.1016/j.jpowsour.2012.07.078
10. Tanuma T, Kawamoto M, Kinoshita S (2017) Effect of properties of hydrophilic microporous layer (MPL) on PEFC performance. *J Electrochem Soc* 164: F499–F503. https://doi.org/10.1149/2.0371706jes
11. Liu CP, Saha P, Huang Y, et al. (2021) Measurement of contact angles at carbon fiber–water–air triple-phase boundaries inside gas diffusion layers using X-ray computed tomography. *ACS Appl Mater Interfaces* 13: 20002–20013. https://doi.org/10.1149/MA2021-0127968mtgabs
12. Yu S, Li X, Liu S, et al. (2014) Study on hydrophobicity loss of the gas diffusion layer in PEMFCs by electrochemical oxidation. *RSC Adv* 4: 3852–3856. https://doi.org/10.1039/C3RA45770B
13. Borup R, Meyers J, Pivovar B, et al. (2007) Scientific aspects of polymer electrolyte fuel cell durability and degradation. *Chem Rev* 107: 3904–3951. https://doi.org/10.1021/cr0501821
14. Chia CH, Munroe P, Joseph SD (2012) Microstructural characterization of white charcoal. *Microsc Microanal* 18: 1562–1563. https://doi.org/10.1016/j.jaap.2014.06.009

15. Rhim Y-R, Zhang D, Fairbrother DH, et al. (2010) Changes in electrical and microstructural properties of microcrystalline cellulose as function of carbonization temperature. *Carbon* 48: 1012–1024. https://doi.org/10.1016/j.carbon.2009.11.020
16. Syarif N, Rohendi D, Haryati S, et al. (2020) Preparing of carbon nanodots from binchotan carbon by electrochemically sonification and dialysis. *IOP Conf Ser Mater Sci Eng* 796: 012057. https://doi.org/10.1088/1757-899X/796/1/012057
17. Park S, Popov BN (2011) Effect of a GDL based on carbon paper or carbon cloth on PEM fuel cell performance. *Fuel* 90: 436–440. https://doi.org/10.1016/j.fuel.2010.09.003
18. Adhiyanti N, Rohendi D, Syarif N, et al. (2020) Preparation and characterization of Ti-Co/C catalyst for PEMFC cathode. *Indones J Fundam Appl Chem* 6: 109–114. https://doi.org/10.24845/ijfac.v6.i3.109
19. Niblett D, Niasar V, Holmes S (2020) Enhancing the performance of fuel cell gas diffusion layers using ordered microstructural design. *J Electrochem Soc* 167: 013520. https://doi.org/10.1149/2.0202001JES
20. Park I-S, Li W, Manthiram A (2010) Fabrication of catalyst-coated membrane-electrode assemblies by doctor blade method and their performance in fuel cells. *J Power Sources* 195: 7078–7082. https://doi.org/10.1016/j.jpowsour.2010.05.004
21. Vadhva P, Hu J, Johnson MJ, et al. (2021) Electrochemical impedance spectroscopy for all solid state batteries: Theory, methods and future outlook. *Chem Electro Chem* 8: 1930–1947. https://doi.org/10.1002/celc.202100108
22. Hoseinzadeh S, Ghasemiasl R, Bahari A, et al. (2017) n-type WO3 semiconductor as a cathode electrochromic material for ECD devices. *J Mater Sci Mater Electron* 28: 14446–14452. https://doi.org/10.1007/s10854-017-7306-7
23. Atteya MA, Salem MAM, Hegazy D, et al. (2016) Image analysis for particle size recognition of bioprocesses in liquid environment. *Asian J Appl Sci* 9: 170–177. https://doi.org/10.3923/ajaps.2016.170.177
24. Gramsch E, Reyes F, Oyola P, et al. (2014) Particle size distribution and its relationship to black carbon in two urban and one rural site in Santiago de Chile. *J Air Waste Manag Assoc* 64: 785–796. https://doi.org/10.3923/ajaps.2016.170.177
25. Sakho EHM, Allahyari E, Oluwafemi OS, et al. (2017) Dynamic light scattering (DLS). *Therm Rheol Meas Tech Nanomater Charact* 2017: 37–49. https://doi.org/10.1016/B978-0-323-46139-9.00002-5
26. Wei Y, Li C, Wang Y, et al. (2012) Regenerating sodium hydroxide from the spent caustic by bipolar membrane electrodialysis (BMED). *Sep Purif Technol* 86: 49–54. https://doi.org/10.1016/j.seppur.2011.10.019
27. Spiegel C (2021) Introduction to Electrolyzers—Fuel Cell Store. Available from: https://www.fuelcellstore.com/blog-section/introduction-to-electrolyzers.
28. Cuéllar-Herrera L, Arce-Estrada E, Romero-Serrano A, et al. (2021) Microwave-assisted synthesis and characterization of γ-MnO2 for high-performance supercapacitors. *J Electron Mater* 50: 5577–5589. https://doi.org/10.1007/s11664-021-09098-x
29. Lukács Z, Kristóf T (2020) A generalized model of the equivalent circuits in the electrochemical impedance spectroscopy. *Electrochimica Acta* 363: 137199. https://doi.org/10.1016/j.electacta.2020.137199

30. Gómez-Aguilar JF, Escalante-Martínez JE, Calderón-Ramón C, et al. (2016) Equivalent circuits applied in electrochemical impedance spectroscopy and fractional derivatives with and without singular kernel. *Adv Math Phys* 2016: 1–15. https://doi.org/10.1155/2016/9720181
31. Holm S, Holm T, Martinsen ØG (2021) Simple circuit equivalents for the constant phase element. *PLOS ONE* 16: e0248786. https://doi.org/10.1371/journal.pone.0248786
32. Popova AN (2017) Crystallographic analysis of graphite by X-Ray diffraction. *Coke Chem* 60: 361–365. https://doi.org/10.3103/S1068364X17090058
33. Berti D, Palazzo G (2022) Colloidal foundations of nanoscience. 2014: 267–273. https://doi.org/10.1016/B978-0-444-59541-6.09995-1
34. Danaei M, Dehghankhold M, Ataei S, et al. (2018) Impact of particle size and polydispersity index on the clinical applications of lipidic nanocarrier systems. *Pharmaceutics* 10: 57. https://doi.org/10.3390/pharmaceutics10020057
35. Mudalige T, Qu H, Van Haute D, et al. (2019) Characterization of nanomaterials. *Nanomater Food Appl* 2019: 313–353. https://doi.org/10.1016/B978-0-12-814130-4.00011-7
36. Zhang L, Pan Z, Huang Q (2013) Effect of primary particle size on colloidal stability of multiwall carbon nanotubes. *Water Sci Technol* 68: 2249–2256. https://doi.org/10.2166/wst.2013.489
37. Bartley PC, Jackson BE, Fonteno WC (2019) Effect of particle length to width ratio on sieving accuracy and precision. *Powder Technol* 355: 349–354. https://doi.org/10.1016/j.powtec.2019.07.016
38. Kitahara T, Nakajima H, Mori K (2012) Hydrophilic and hydrophobic double microporous layer coated gas diffusion layer for enhancing performance of polymer electrolyte fuel cells under no-humidification at the cathode. *J Power Sources* 199: 29–36. https://doi.org/10.1016/j.jpowsour.2011.10.002
39. Mei B-A, Munteshari O, Lau J, et al. (2018) Physical interpretations of Nyquist plots for EDLC electrodes and devices. *J Phys Chem C* 122: 194–206. https://doi.org/10.1021/acs.jpcc.7b10582
40. Herrera Hernández H, Ruiz Reynoso AM, Trinidad González JC, et al. (2020) Electrochemical impedance spectroscopy (EIS): A review study of basic aspects of the corrosion mechanism applied to steels. In: El-Azazy M, Min M, Annus P. *Electrochemical Impedance Spectroscopy.* https://doi.org/10.5772/intechopen.94470
41. Pecqueur S, Lončarić I, Zlatić V, et al. (2019) The non-ideal organic electrochemical transistors impedance. *Org Electron* 71: 14–23. https://doi.org/10.1016/j.orgel.2019.05.001f
42. Naftalovich R, Naftalovich D, Greenway F (2016) Polytetrafluoroethylene ingestion as a way to increase food volume and hence satiety without increasing calorie content. *J Diabetes Sci Technol* 10: 971–976. https://doi.org/10.1177/1932296815626726
43. Aoyama Y, Tabe Y, Nozaki R, et al. (2018) Analysis of water transport inside hydrophilic carbon fiber micro-porous layers with high-performance operation in PEFC. *J Electrochem Soc* 165: F484–F491. https://doi.org/10.1149/2.0801807jes

AIMS Press

Gas diffusion layer from Binchotan carbon and its electrochemical properties for supporting electrocatalyst in fuel cell

ORIGINALITY REPORT

16%	15%	6%	1%
SIMILARITY INDEX	INTERNET SOURCES	PUBLICATIONS	STUDENT PAPERS

PRIMARY SOURCES

1	www.researchgate.net Internet Source	9%
2	ouci.dntb.gov.ua Internet Source	3%
3	aidic.it Internet Source	1%
4	journal.unnes.ac.id Internet Source	1%
5	Minkmas V. Williams, Eric Begg, Leonard Bonville, H. Russell Kunz, James M. Fenton. "Characterization of Gas Diffusion Layers for PEMFC", Journal of The Electrochemical Society, 2004 Publication	1%
6	Zhang, S.. "A review of accelerated stress tests of MEA durability in PEM fuel cells", International Journal of Hydrogen Energy, 200901 Publication	1%

Exclude quotes	On	Exclude matches	< 1%
Exclude bibliography	On		